Aquatic Toxicology 225 (2020) 105552

Contents lists available at ScienceDirect

Aquatic Toxicology

journal homepage: www.elsevier.com/locate/aqtox

Physiological and metabolic responses to hypersalinity reveal interpopulation tolerance in the green macroalga *Ulva compressa* with different pollution histories

Pamela T. Muñoz[a,b,c,g], Fernanda Rodríguez-Rojas[a,g], Paula S.M. Celis-Plá[a,g], Lorena Méndez[a,d], Denise Pinto[a,b,g], Diego Pardo[a,e,g], Fabiola Moenne[a,g], José Luis Sánchez-Lizaso[f], Claudio A. Sáez[a,g,*]

[a] Laboratory of Aquatic Environmental Research, Centro de Estudios Avanzados, Universidad de Playa Ancha, Viña del Mar, Chile
[b] Doctorado Interdisciplinario en Ciencias Ambientales, Facultad de Ciencias Naturales y Exactas, Universidad de Playa Ancha, Valparaíso, Chile
[c] Doctorado en Ciencias del Mar y Biología Aplicada, Departamento de Ciencias del Mar y Biología Aplicada, Universidad de Alicante, Alicante, Spain
[d] Carrera de Biología Marina, Facultad de Ciencias del Mar y Recursos Naturales, Universidad de Valparaíso, Viña del Mar, Chile
[e] Carrera de Ingeniería Civil Ambiental, Facultad de Ingeniería, Universidad de Playa Ancha, Valparaíso, Chile
[f] Departamento de Ciencias del Mar y Biología Aplicada, Universidad de Alicante, Alicante, Spain
[g] ENVIRONMENTAL HUB UPLA, Universidad de Playa Ancha, Valparaíso, Chile

ARTICLE INFO

Keywords:
Osmotic stress
Chlorophyta
Desalination
Reactive oxygen species
Transcriptomics
Intraspecific

ABSTRACT

There is scarce investigation addressing interpopulation tolerance responses to address the influence of a history of chronic stress exposure, as that occurring in polluted environments, in photoautotrophs. We evaluated eco-physiological (photosynthetic activity) and metabolic (oxidative stress and damage) responses of two populations of green macroalga *Ulva compressa* from polluted (Ventanas) and non-polluted (Cachagua) localions of central Chile, and exposed to controlled hypersalinity conditions of 32 (control), 42, 62 and 82 psu (practical salinity units) for 6 h, 48 h and 6 d. Both primary production (ETR_{max}) and photosynthetic efficiency (α_{ETR}) were generally higher in the population from Cachagua compared to Ventanas at all times and salinities. Moreover, at most experimental times and salinities the population from Ventanas had greater levels of H_2O_2 and lipid peroxidation that individuals from Cachagua. Total ascorbate was higher in the population of Cachagua than Ventanas at 42 and 82 psu after 6 and 48 h, respectively, while at 6 d concentrations were similar between both populations at all salinities. Total glutathione was greater in both populations after 6 h at all salinities, but at 48 h its concentrations were higher only in the population from Cachagua, a trend that was maintained at 6 d under 82 psu only. Reduced and oxidized ascorbate (ASC and DHA, respectively) and glutathione (GSH and GSSG, respectively) demonstrated similar patterns between *U. compressa* populations, with an increase oxidation with greater salinities but efficient recycling to maintain sufficient batch of ASC and GSH. When assessing the expression of antioxidant enzymes catalase (*CAT*), superoxide dismutase (*SOD*) and dehydroascorbate reductase (*DHAR*), while the population of Ventanas displayed a general trend of upregulation with increasing salinities along the experiments, *U. compressa* from Cachagua revealed patterns of downregulation. Results demonstrated that although both populations were still viable after the applied hypersalinities during all experimental times, biological performance was usually more affected in the population from the Ventanas than Cachagua, likely due to a depressed baseline metabolism after a long history of exposition to environmental pollution.

1. Introduction

Salinity is a determinant abiotic factor for growth and development in macroalgae; changes in salinity in the marine environment can occur due to natural conditions such as estuarine or tidal range, and also anthropic activities as desalinization brine discharges (Rybak, 2018; Luo and Liu, 2011; Sola et al., 2019b, a; Fernández-Torquemada et al., 2009). Hypersalinity can produce osmotic stress, manifested in aspects such as cell dehydration, Na^+ and Cl^- accumulation, and in changes in K^+/Na^+ and Ca^{2+}/Na^+ ratios due to selective uptake and organic

* Corresponding author at: ENVIRONMENTAL HUB UPLA, Universidad de Playa Ancha, Valparaíso, Chile
E-mail address: claudio.saez@upla.cl (C.A. Sáez).

https://doi.org/10.1016/j.aquatox.2020.105552
Received 12 March 2020; Received in revised form 12 May 2020; Accepted 16 June 2020
Available online 25 June 2020
0166-445X/

osmolytes accumulation (Kirst, 1990; Kumar et al., 2014; Marín-Guirao et al., 2013; Sandoval-Gil et al., 2014; Garrote-Moreno et al., 2015). This can lead to perturbations in enzymatic processes, changes in the membrane potential and toxic responses due to overproduction of reactive oxygen species (ROS) (Sampath-Wiley et al., 2008; Kumar et al., 2014).

Oxidative stress is caused due an imbalance between ROS excess and cellular antioxidant capacity (Gill and Tuteja, 2010; Hajiboland, 2014). ROS are mainly produced by electron transport flow within the chloroplast and mitochondria, process that under environmental stress can lead to disruption and induce overproduction of ROS such as superoxide anion ($O_2^{\cdot -}$), hydrogen peroxide (H_2O_2) and hydroxyl radical (·OH), among others (Imlay, 2003; Kumar et al., 2014). Subsequent oxidation of target macromolecules includes lipids, proteins and nucleic acids and, in severe cases, inhibition and/or destruction of organellar function (e.g. photosynthetic apparatus malfunction) (Gill and Tuteja, 2010; Kumar et al., 2014). Decrease or inhibition in photosynthesis occurs due chlorophyll degradation, D1 protein oxidation in the photosystem II reaction center complex and perturbation in electron transport chains (Xia et al., 2004; Hajiboland, 2014). On the other hand, over accumulation of ROS stimulate the activation of antioxidant defenses, based mainly in the synthesis of metabolites of and activities of enzymes with antioxidant proprieties (Moenne et al., 2016; Sáez et al., 2015c, a; Sáez et al., 2015b; Rodríguez-Rojas et al. 2019). The small water- soluble molecules ascorbate and glutathione, synthesized during the Foyer–Halliwell–Asada cycle, participate as ROS scavengers and reduction of oxidized molecules (Foyer and Noctor, 2011; Asada, 1999). On the other hand, both superoxide dismutase (SOD) and catalase (CAT) have been identified as core antioxidant enzymatic systems dismutating $O_2^{\cdot -}$ and H_2O_2, respectively (Ślesak et al., 2016). In addition, other enzymes, such as ascorbate peroxidase (APX) reduces H_2O_2 through the oxidation of reduced ascorbate (ASC) forming monodehydroascorbate (MDHA) and subsequently dehydroascorbate (DHA), the most common form of oxidised ascorbate (Foyer and Noctor, 2011; Asada, 1999). Then, dehydroascorbate reductase (DHAR) reduce DHA to ASC using reduced glutathione (GSH) as substrate; finally, glutathione reductase (GR) reduces oxidized glutathione (GSSG) using NADP(H) as an electrons donor (Moenne et al., 2016; Foyer and Noctor, 2011; Asada, 1999). Different records account for the induction of antioxidant defenses under hypersalinity in macroalgae. For instance, investigations carried out by Lu et al. (2006) in *Ulva fasciata* showed decreasing of photosynthesis by hypersalinity (90 psu) after 4 days of exposition would lead to an accumulation of H_2O_2 in the talus inducing oxidative stress observed by lipid peroxidation quantification and increasing of antioxidant defenses as ASC and GSH. Beside was observed increasing enzymes as CAT and others derived of glutathione-ascorbate cycle as APX, glutathione reductasa GR and monohydroascorbate reductase (MDHAR). Luo and Liu (2011) registered a rapid accumulation of GSH and an increase activity of CAT, SOD, APX and GR when *U. prolifera* was exposed to hypersalinity (60 psu) for 6 days. Molecular aspects of gene transcription related to antioxidant defense showed that *U. fasiata* has a peak regulation of gene expression of *MnSOD*, *APX* and *GR* after 3 h of exposition to hypersalinity conditions (90 psu) (Sung et al., 2009). However, to the extent of our knowledge, there is no published information regarding intraspecific antioxidant responses in macroalgae species, and certainly not in populations with different histories of exposure to environmental pressures.

Categorized in more than 120 taxa and belonging to the group of Chlorophyta, species of the genus *Ulva* inhabit intertidal environments with high salinity variations (Rybak, 2018). *U. compressa* is a cosmopolitan, dominant and opportunistic macroalga, capable of surviving in highly polluted environments (Rybak, 2018; Ogawa et al., 2013; Sampath-Wiley et al., 2008). In addition, the low morphological complexity and success to colonize different environments of *U. compressa* has stimulated its use as model to understand abiotic stress in green macroalgae (Moenne et al., 2016). In this context, *U. compressa* has been widely used to evaluate the effects of metals such copper excess, under laboratory and field evaluations (Celis-Plá et al., 2019; Rodríguez-Rojas et al., 2019; Mellado et al., 2012; Ratkevicius et al., 2003). Although several studies report the potential mechanisms of this macroalga to cope with different abiotic stressors, there is still no published information on the potential tolerance responses to different salinity regimes in *U. compressa*, nor addressing interpopulation potential variations.

In this study, we evaluated different physiological and metabolic responses to a range of hypersalinities in two *U. compressa* populations inhabiting sites with distinct pollution histories. Thus, providing insights concerning cellular and molecular mechanisms driving hypersaline stress tolerance in a chronically anthropogenic-mediated stressed population and another subject to minimum impacts.

2. Materials and methods

2.1. Study sites, macroalgae collection and experimental design

Ventanas (32°43′S 71°29′W) is a polluted industrial location belonging to the urban district of Quintero and Puchuncaví, Valparaiso province of central Chile. This district has a population of near 43.400 inhabitants, with surface area of 450 km^2. Created in the 1950's, is considered the main and most important industrial area of central Chile. Different sources of contamination are present in the area, such as cooper and hydrocarbons refineries, dock and port facilities and a thermoelectric, among others, having visible and historical negative effects on terrestrial and marine ecosystems (Tume et al., 2019; Sáez et al., 2015a, a; Sáez et al., 2012b; Neaman et al., 2009). North from Ventanas (30 km), is found Cachagua (32°34′S 71°26′W), a small recreational beach town with no history of any important human impacts.

Adult individuals of two populations of *U. compressa* were randomly collected through the vertical gradient of the intertidal zone in Ventanas and Cachagua. *U. compressa* was stored in a cooler and immediately transported to a culture chamber for acclimatization for 48 h (h) in controlled laboratory conditions. These included constant aeration, temperature of 15 ± 1 °C, light (120 μmol photons m^{-2} s^{-1}) and a photoperiod 12:12 light/dark cycle. After acclimatization, hypersaline treatments consisted in: 32 (control treatment), 42, 62 and 82 psu (practical salinity units). It is important to mention that control conditions were selected upon known average salinities in seawater of central Chile (Sievers and Vega, 2000), which was confirmed *in situ* at the *U. compressa* collection sites with a multiparametrical probe (Hanna model HI 98194). Likewise, increased salinities were chosen based in average salinities recorded in intertidal pools described elsewhere (Tine et al., 2008; Vargas-Chacoff et al., 2015). Salinities were obtained supplementing autoclaved filtered seawater with artificial sea salts (Instant Ocean ®), monitored with the multiparametrical probe. One hundred mg of *U. compressa* were distributed separately in 500 mL lid-free polycarbonate containers, in triplicates for each condition. Subsamples were collected at 6 h, 48 h and 6 days (d). Some were used for photosynthetic performance analyses and the rest immediately frozen in liquid nitrogen and stored at −80 °C for further analyses.

2.2. Photosynthetic performance

Photosynthetic measurements were performed throughout the course of the experiments in all treatments, at 6, 48 h and 6 d. Maximum quantum yield of photosystem II (PII; F_v/F_m) was measured using a pulse-amplitude modulated (PAM) chlorophyll α fluorometer (JUNIOR PAM, blue version; Walz GmbH, Effeltrich, Germany) with WinControl-3.2 software. This parameter was measured according to Schreiber et al. (1995) : F_v/F_m; $F_v = F_m - F_0$, being F_0 basal fluorescence after maintaining algae by 15 min in the dark and F_m maximum fluorescence after short saturation light pulse (> 1500 μmol m^{-2} s^{-1}, 0.8 s) measured by blue light (λ_{max} = 445 nm) measuring. The electron

transport rate (ETR) was determined after 20 s exposure to twelve steps increasing actinic light intensities (from 0 to 1500 μmol photons m^{-2} s^{-1}). ETR was calculated according to Schreiber et al. (1995):

ETR (μmol electrons $m^{-2}s^{-1}$): $(\Delta F/F'_m) \times E \times A \times F_{II}$;

Where $\Delta F/F'_m$ is the effective quantum yield, being $\Delta F = F'_m - Ft$ (Ft is the intrinsic fluorescence of alga incubated in light and F'_m is the maximal fluorescence reached after a saturation pulse of alga incubated in light); E is the incident photosynthetically active radiation (PAR) irradiance on the alga expressed in μmol photons $m^{-2}s^{-1}$; A is the absorptance defined as fraction of incident irradiance that is absorbed (Figueroa et al., 2003) by the algae (measured with Apogee instrument model MQ-200); and FII is the fraction of chlorophyll related to PSII (400–700 nm) being 0.5 in green macroalgae (Figueroa et al., 2014). And the initial slope of ETR vs irradiance function (α_{ETR}) as estimator of photosynthetic efficiency were obtained from the tangential function reported Eilers and Peeters (1988). The saturation irradiance for ETR (Ek_{ETR}) was calculated from the intercept between ETR_{max} and α_{ETR}. Non-photochemical quenching (NPQ) was calculated according to Schreiber et al. (1995):

$$NPQ = (F_m - F'_m)/ F'_m$$

Maximal NPQ (NPQ_{max}) and the initial slope of NPQ vs. irradiance function (αNPQ) were obtained from the tangential function of NPQ vs irradiance function according to Eilers and Peeters (1988).

2.3. Quantification of hydrogen peroxide (H_2O_2)

H_2O_2 content was determined according to Sergiev et al. (1997) with modifications for *U. compressa*. Briefly, 200 mg of frozen biomass was ground with liquid nitrogen and mixed with 100 μL 0.1 % trichloroacetic acid (TCA), 100 μL 10 mM potassium phosphate buffer (pH 7.0), 100 μL 100 mM EDTA and 500 μL 1 M potassium iodide. The mixture was vortexed for 10 min in darkness at room temperature. The homogenate was centrifuged at 12,000x *g* for 5 min at 4 °C. A volume of 300 μL of supernatant was placed in 96-well microplate reader (SpectroStar Nano, BMG LABTECH) and absorbance was measured at 390 nm. Commercial H_2O_2 (Sigma Aldrich Merck, St Louis, MO, USA) was used for standard curves. Data was normalized against proteins concentrations measured by the Bradford method (Bradford, 1976).

2.4. Quantification of thiobarbituric acid reactive substances (TBARS)

TBARS, as a proxy for lipid peroxidation, were determinated according to Sáez et al. (2015c) with modifications for *U. compressa*. Frozen biomass was ground (200 mg) with liquid nitrogen and mixed with 300 μL 0.1 % TCA, vortexed by 10 min and centrifuged at 17800x g for 15 min at 4 °C. Then, 200 μL of supernatant was mixed with 200 μL 0.5 % thiobarbituric acid (TBA) and incubated for 45 min at 95 °C. A volume of 200 μL of supernatant was measured at 532 nm in microplate reader. Commercial malondialdehyde (MDA, Sigma Aldrich Merck) was used for constructing standard curves. Data was normalized against protein concentrations measured by the Bradford method (Bradford, 1976).

2.5. Quantification of ascorbate (ASC) and dehydroascorbate (DHA)

Concentrations of ASC and DHA were determined using the FRAP reagent according to Sáez et al. (2015c) with modifications for *U. compressa*. The frozen biomass was ground (200 mg) with liquid nitrogen and mixed with 600 μL of 0.1 M HCl, vortexed for 10 min at room temperature and then centrifuged at 17,800x g for 15 min at 4 °C. To determinate ASC content, 10 μL of extract was placed in microplate that contained 290 μL of FRAP reagent (300 mM pH 3.6 sodium acetate buffer, 20 mM $FeCl_3$ and 10 mM 2,4,6-tripyridyl-s-triazine (TPTZ)). The absorbance was determined at 593 nm in the microplate reader. To determinate total ascorbate (ASC + DHA) 25 μL of extract was incubated with 2.5 μL mL 100 mM 1,4- dithiothreitol (DTT) for 1 h at room temperature. The reaction was stopped with 5% N-ethylmaleimide and 10 μL of this extract was placed in the microplate reader containing 290 μL FRAP reagent. DHA was obtained by subtracting ASC content from total ascorbate. The absorbance was determined at 593 nm, in the same manner as for ASC. Commercial L-ascorbate (Sigma Aldrich Merck) was used for the standard curve. Data was normalized against proteins concentrations measured by the Bradford method (Bradford, 1976).

2.6. Quantification of reduced (GSH) and oxidized (GSSG) glutathione

GSH and GSSG were determinate according Sáez et al. (2015c) with modification for *U. compressa*. The frozen biomass was ground (200 mg) with liquid nitrogen, mixed with 500 μL 0.1 M HCl, vortexed for 10 min at temperature room and then centrifuged for 15 min at 7400x g at 4 °C. The extract was neutralized with 500 μL of 500 mM sodium phosphate buffer (pH 7.5). To measure total glutathione (GSH + GSSG) 50 μL of the neutralized extract was mixed with 250 μL of "GR" buffer (100 mM sodium phosphate pH 3.6, 0.1 mM EDTA, 0.34 mM NADPH, 0.2 mM Elmann's reagent or DTNB and 0.6 units GR enzyme (Sigma-Aldrich)). The absorbance was measured immediately at 412 nm every 20 s for 5 min. For GSSG quantification, 50 μL of neutralized extract was mixed with 1 μL of 1 M 4-vinylpyridine and incubated for 1 h. Then, 50 μL of the extract was mixed with 250 μL of "GR" buffer and absorbance was read the same way was for total glutathione. GSH was obtained by subtracting GSSG content from total glutathione. Commercial GSH (Sigma Aldrich Merck) was used as standard curve. Data was normalized against proteins concentrations measured by the Bradford method (Bradford, 1976).

2.7. RNA purification cDNA synthesis and qPCR

Genes analyzed corresponded to those encoding for catalase (*CAT*), superoxide dismutase (*SOD*) and dehidroascobate reductase (*DHAR*), and 18S rRNA as housekeeping gene. RNA was obtained from 100 mg of ground tissue of *U. compressa* using the E.Z.N.A. Total RNA Kit I. RNA purity and integrity were determined by 260/280 ratio and electrophoresis in 1 % agarose bleach gel (Aranda et al., 2012), respectively. RNA quantification was carried out using the Quant-iT RiboGreen RNA assay kit (Invitrogen, Waltham, MA, USA) using a QFX Fluorometer (DeNovix, Wilmington, DE, USA).

Synthesis of cDNA was obtained with 500 ng of total RNA and using the ProtoScript First Stand cDNA Synthesis Kit (New England BioLabs, Ipswich, MA, USA), following guidelines of the manufacturer. For the qPCR reactions 50 ng (2 μL) of cDNA were used, 0.25 μM of each primer and the 1X of the Brilliant II SYBR Green QPCR Master Mix (Agilent Technologies, Santa Clara,CA, USA) adjusted to a final volume of 20 μL. Then, the qPCR program was: initial denaturation at 95 °C for 5 min and then 40 cycles of 95 °C for 30 s, 55 °C for 30 s, 72 °C for 40 s, ending with a final extension at 72 °C for 10 min. These reactions were performed in a MIC qPCR Magnetic Induction Cycler (Bio Molecular Systems, Queensland, Australia). Genes analyzed corresponded to those encoding for catalase, *CAT* (forward P: 5′-AGCGGAACAAGTCGGCGG CAA-3′ and reverse P: 5′- CAGCACCATGCGGCCAACGG-3′); superoxide dismutase, *SOD* (forward P: 5′−CCCTGCACCGCCGTCTGTCG-3′ and reverse P: 5′- CGCGCTGCTGATCTTCGGAGCA-3′); and dehydroascorbate reductase, *DHAR* (forward P: 5′- CGCGGACTCCGGCGAC ATCT-3′ and reverse P: 5′- AGCGCTGCGAGCTCCTCTGG). As a reference gene the 18S rRNA subunit was used (forward P: 5′- AATTTG ACTCAACACGGG-3′ and reverse P: 5′- TACAAAGGGCAGGGACG-3′). All primers were obtained from Rodríguez-Rojas et al. (2019). Relative expression analyses were based in the $2^{-\Delta\Delta Ct}$ method using 18S rRNA as housekeeping gene (Livak and Schmittgen, 2001).

2.8. Statistical analyses

Previous to statistical analyses, normality and homogeneity of variances was checked by Shapiro- Wilks and Cochran tests, respectively. To evaluate differences between populations (Cachagua and Ventanas) of *U. compressa* and the effects of salinities (32, 42, 62, 82 psu) on physiological (F_v/F_m, ETR_{max}, α_{ETR}, Ek_{ETR} y NPQ*max*), biochemical (H_2O_2, TBARS, total ascorbate (ASC + DHA) and total glutathione (GSH + GSSG)) and molecular (gene expression *DHAR, CAT, SOD*) parameters, a factorial ANOVA followed by a Student-Neuwman-Keuls –SNK as posteriori test. A level of significance of 95 % confidence interval ($p = 0.05$) was considered. Gene expression dates were transformed to square root before of statistical analyses to normalize the data. These analyses were performed using the software Statistica version 7 (StatSoft Inc., Tulsa, OK, USA) and statistical package SPSS v.21 (IBM, USA). A Principal coordinate ordination (PCO) analyses was applied to identified patterns between the parameters on the basis of an Euclidean distance using PERMANOVA + for PRIMER6 package. For the PCO analyses, H_2O_2, TBARS, ETR_{max}, α_{ETR}, Ek_{ETR}, NPQ*max*, total ascorbate, total glutathione and gene expression *DHAR, CAT* and *SOD*, were incorporated in the analysis.

3. Results

3.1. Photosynthetic responses

Salinity showed no significant effects on photosynthetic inhibition (measured as F_v/F_m) for all experimental times evaluated in both populations from Ventanas and Cachagua of *U. compressa* (data not shown). However, in the ETR_{max}, after 6 h lower ETR_{max} was detected as salinity increased, although with no particular trend between populations (Fig. 1A–C). There was a trend in ETR_{max}, although not significant at 6 h, in which baseline levels at 32 psu were always higher in the Cachagua population in relation to the Ventanas; these then reach similar levels as salinity concentrations increased (Fig. 1A–C). On the other hand, at 6 h, with no significant difference at 42 psu, the tendency was higher photosynthetic efficiency α_{ETR} in the Cachagua population (Fig. 1D). Similar responses were observed at 48 h and 6 d, but salinity had a significant effect in decreasing α_{ETR} at 62 and above in Cachagua's population (Fig. 1E and F). No clear patterns could be observed along experimental times and salinity concentrations between populations in the case of Ek_{ETR} and NPQ_{max} (Supplementary Fig. 1**D-F**).

3.2. Quantification of H_2O_2

After 6 h, although not always significant, there was a marked trend that showed an increased accumulation of H_2O_2 in the population from Ventanas population compared to Cachagua across salinity treatments (Fig. 2A). At 48 h and 6d, there was only a significant increase in H_2O_2 at 42 psu compared to controls; however, beyond this salinity exposure, H_2O_2 returns to baseline concentrations (Fig. 2B and C).

3.3. Quantification of TBARS

Control salinity did not show differences in TBARS between both populations at all experimental times (Fig. 3A–C). As a general trend among times, at 62 psu and beyond TBARS levels were higher in the *U. compressa* population from Ventanas compared to Cachagua (Fig. 3A–C). Only in the case of the population at Ventanas at 6 d it was observed a significant increase in TBARS upon salinity levels, although reaching the 82 psu TBARS returned to levels similar to controls (Fig. 3C).

3.4. Glutathione and ascorbate levels

At 6 h, no trends were observed in total ascorbate (ASC + DHA) between populations (Fig. 4A). No significant differences or even lower levels were detected in total ascorbate upon increasing salinities in the population from Ventanas at all experimental times (Fig. 4A-C). For *U. compressa* from Cachagua, at 6 h suffered a significant increase in total ascorbate at 42 psu, but at higher salinities it decreased even below control levels (Fig. 4A). At 48 h and 6 d, important increases in total ascorbate were observed mainly at 82 psu (Fig. 4B, C). Inverted patterns in the relation ASC/DHA could be observed between populations subject to increasing salinities. The population from Ventanas starts (6 h) with higher levels of DHA in relation to ASC at control conditions, as time advances (48 h and 6 d) this pattern moves towards the highest salinity (82 psu); the population from Cachagua, instead, follows the opposite salinity-trend in time (Fig. 4A–C).

After 6 h, total glutathione (GSH + GSSG) was significantly higher in the population from Cachagua exposed to 42, 62 and 82 psu in relation to controls, whereas this occurred in *U. compressa* at 62 and 82 psu (Fig. 5A). At 48 h, there is a trend of significant increase in total glutathione in the population from Cachagua, with the highest concentrations at 82 psu (Fig. 5B). In total glutathione from Ventanas at 48 h a significant decrease was observed only at 42 psu (Fig. 5B). After 6 d,

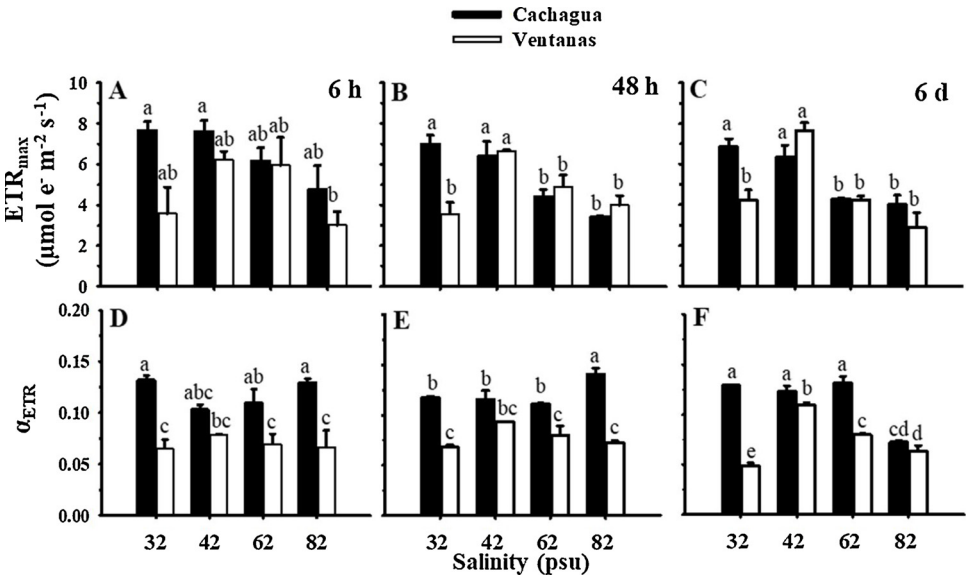

Fig. 1. Maximum electrons transport rate (ETR_{max}) and photosynthetic efficiency (α_{ETR}) of *U. compressa* populations from Cachagua (black bars) and Ventanas (white bars) exposed to different salinities. Both populations were exposed to: 32 (control), 42, 62 and, 82 psu. Samples were analyzed after 6 h (A), 48 h (B) and 6d (C). Data correspond to mean ± SE ($n = 3$). Letters represent statistical differences at 95 % confidence interval (SNK test, $p < 0.05$).

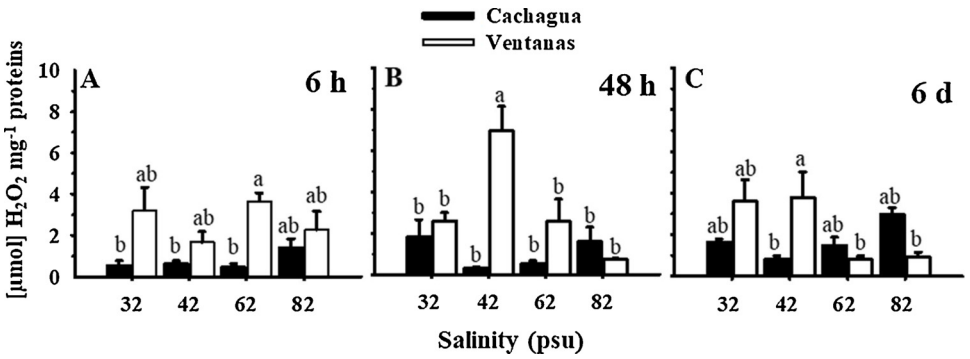

Fig. 2. Hydroxide peroxide (H_2O_2) content in *U. compressa* populations from Cachagua (black bars) and Ventanas (white bars) localities exposed to different salinities. Both populations were exposed to: 32 (control), 42, 62 and 82 psu. Samples were analyzed after 6 h (A) and 48 h (B) and 6d (C). Data correspond to mean ± SE (n = 3). Letters represent statistical differences at 95 % confidence interval (SNK test, $p < 0.05$).

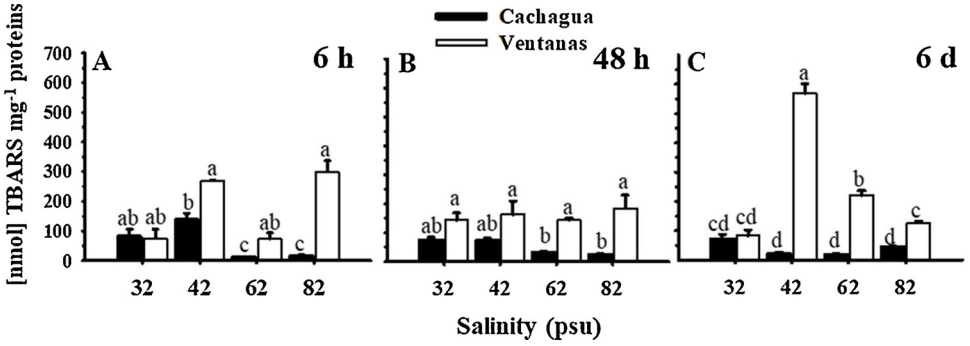

Fig. 3. Thiobarbituric acid reactive subtances (TBARS) in *U. compressa* populations from Cachagua (black bars) and Ventanas (white bars) exposed to different salinities. Both populations were exposed: 32 (control), 42, 62, and 82 psu. Samples were analyzed after 6 h (A) and 48 h (B) and 6d (C). Data correspond to mean ± SE (n = 3). Letters represent statistical differences at 95 % confidence interval (SNK test, $p < 0.05$).

total glutathione from Cachagua population suffered a great increase at 32 and 82 psu, while it decreased significantly at 42 and 62 psu (Fig. 5C). On the other hand, Ventanas *U. compressa* remained at low levels during all salinities, except at 42 psu (Fig. 5C). Tendencies in GSH/GSSG were alike between populations across experimental times, with more than 85 % of the total glutathione as GSH (Fig. 5A–C); the latter was less evident in the population from Cachagua at 48 h, but still GSH levels were always higher than those measured for GSSG (Fig. 5B).

3.5. Oxidative stress-related genes expression

Analyses of relative expression of genes related to oxidative stress showed different patterns in response to times and salinities in both populations. At 6 h, *SOD* was up-regulated in all hypersalinity conditions in the population from Ventanas, whereas the Cachagua's did not show changes in relative expression compared to control salinity (Fig. 6A). In contrast, *SOD* expression showed a marked down-regulation after 48 h in both populations, although repression was greater in the population from Cachagua, specifically at 42 and 62 psu, (Fig. 6B). After 6 d, *SOD* remained inhibited in the population from Cachagua at all salinities; however, it showed a small but significant increase at 42 and 62 psu in the Ventanas population (Fig. 6C). On the other hand, *CAT* displayed downregulation at 42 psu for both population and a tendency for upregulation at higher salinities (Fig. 6D). At 48 h, *CAT* was down-regulated in all salinities except in the population of Cachagua at 82 psu, although without significant differences with the rest of the treatments in the individuals from this location (Fig. 6E). After 6d, *CAT* was significantly up-regulated in the population from Ventanas at 42 and 82 psu, while in *U. compressa* from Cachagua downregulation remained at 42 and 62 psu, although with a slight up-regulation at 82 psu (Fig. 6F). Finally, at 6 h *DHAR* was up-regulated only in Ventanas' and Cachagua's population at 42 and 62 psu, respectively (Fig. 6G). At 48 h, *DHAR* was strongly down-regulated in the population from Cachagua, and also in the population of Ventanas at 42 and 82 psu treatments, although the latter with higher levels of expression than *U. compressa* from Cachagua; at this time-period, DHAR was only upregulated in the population from Ventanas at 62 psu (Fig. 6H). Conversely, at 6 d *DHAR* displayed a significant upregulation in both populations of *U. compressa*, especially at 42 psu, excepting at 62 psu in the population from Cachagua which evidenced a great downregulation (Fig. 6I).

3.6. Principal coordinate ordination (PCO) analyses

The PCO analyses used the whole physiological (including Ek_{ETR} and NPQ_{max}), Biochemical and molecular data presented. The clusters of the measured parameter were organized upon populations (Fig. 7). The PCO showed evident clusters differentiating the populations of

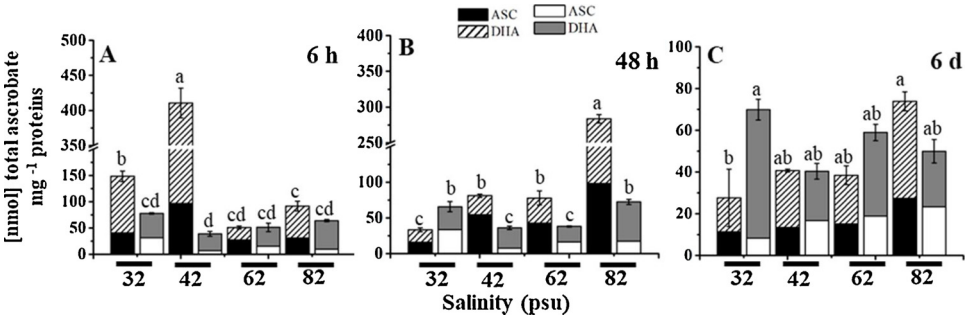

Fig. 4. Total ascorbate (ASC + DHA) in *U. compressa* populations from Cachagua (black (ASC) and striped (DHA) bars) and Ventanas (white (ASC) and grey (DHA) bars) exposed to different salinities. Both populations were exposed to: 32 (control), 42, 62 and 82 psu. Samples were analyzed after 6 h (A) and 48 h (B) and 6d (C). Data correspond to mean ± SE (n = 3). Letters represent statistical differences at 95 % confidence interval (SNK test, $p < 0.05$).

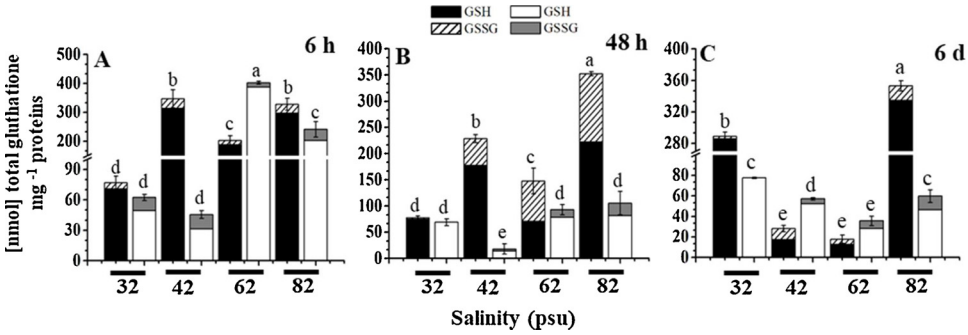

Fig. 5. Total glutathione (GSH + GSSG) in *U. compressa* populations from Cachagua (black (GSH) and striped (GSSG) bars) and Ventanas (white (GSH) and grey (GSSG) bars) exposed to different salinities. Both populations were exposed to hypersalinity: 32 (control), 42, 62 and 82 psu. Samples were analyzed after 6 h (A), 48 h (B) and 6 d (C). Data correspond to mean ± SE (n = 3). Letters represent statistical differences at 95 % confidence interval (SNK test, $p < 0.05$).

Ventanas and Cachagua upon the parameters determined (Fig. 7). Photosynthetic responses were grouped, in agreement with the same pattern all times in both populations.

4. Discussion

In this research, two population of *U. compressa* from polluted (Ventanas) and non-polluted (Cachagua) localities were exposed to hypersalinity conditions (42, 62 and 82 psu), in order to characterize physiological and metabolic responses in the context of potential intraspecific differences mediated by a history of survival under anthropogenic environmental pressures. Our results showed a marked difference in responses observed between the two populations (see multivariate analysis). A trend of lower ETR_{max} and α_{ETR} was observed in both populations upon increasing salinities, although while in the population from Cachagua this pattern was only visible at the highest levels (82 psu), in the ecotype from Ventanas it started at 62 psu. Investigations by Xia et al. (2004) showed that the stress produced by salinity excess can produce the inactivation of active reaction centers of PSII in *U. lactuca,* resulting in a decrease of fluorescence emission, upon which parameters as ETR_{max} and α_{ETR} are estimated. Moreover, the red alga *Gelidium amansii* exposed for 10 days to increased salinities from 32 to 35 psu showed a decrease in fluorescence through efficiency (ψ_o) and quantum yield of electron transport (φ_{EO}), together with lower levels of pigments (chlorophyll *a*, carotenoid and phycobiliproteins); these authors suggested that hypersalinity can cause the blockage of electron transport transferring excess energy to oxygen, over-producing ROS, which subsequently facilitated the oxidation of pigments and affected photosynthetic activity (Li et al., 2016). In spite of the latter, it appears that the effects of hypersalinity can be even an intra-specific feature in green macroalgae, as observed in *U. compressa*, and eventually be influenced by a history of exposure to environmental stress.

Although there was no significant differences in H_2O_2 levels between both populations for most times and salinities, there was a trend showing a higher accumulation of H_2O_2 in the population of *U. compressa* from Ventanas, especially at 42 psu after 48 h; however, this was not observed at other hypersalinity conditions, where H_2O_2 returned nearly baseline levels. This pattern was also linked to higher levels of TBARS in the population from Ventanas, a proxy for lipid peroxidation, although apparently having later effects observable at 6 d of exposure to 42 psu. This data at least, at late exposure of 6 d, is in agreement with potential conversion of H_2O_2 to hydroxyl radicals ($O^{\cdot}H$) through Fenton reaction, which can rapidly increase levels of lipid peroxidation (Imlay, 2003). In this context, Luo and Liu (2011) reported that the increment of H_2O_2 might followed by an increase in lipid peroxidation in *U. prolifera* when exposed to 60 psu compared to controls at 30 psu. Furthermore, the latter authors observed that high levels of H_2O_2 were linked to a decrease in photosynthetic activity as a consequence of

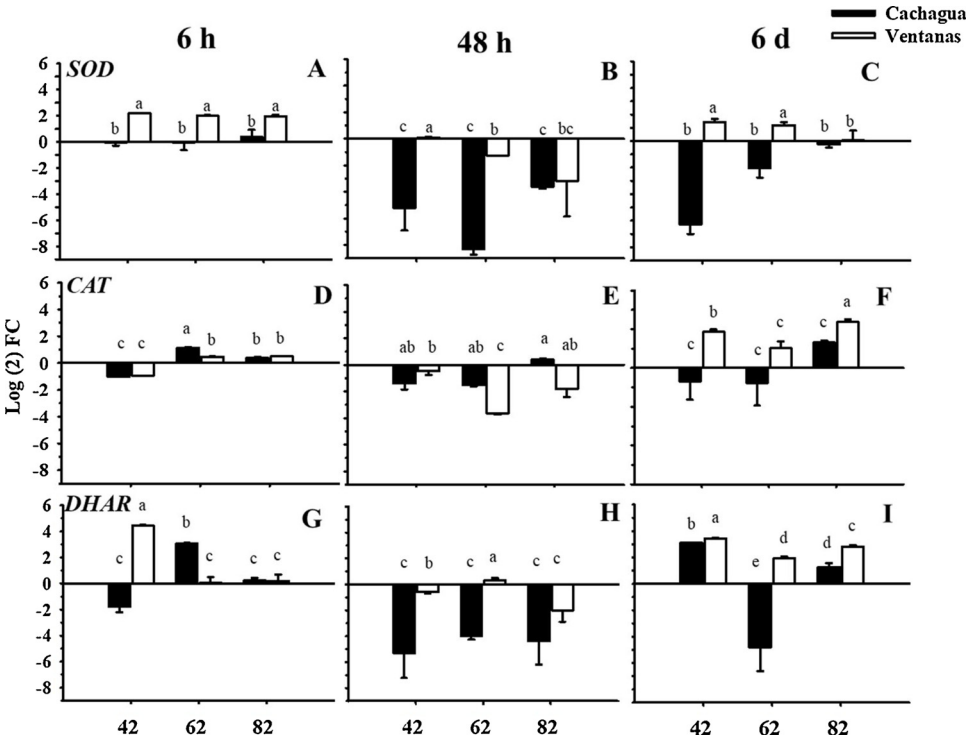

Fig. 6. Relative expression of the genes related to oxidative stress response in *U. compressa* populations from Cachagua (black bars) and Ventanas (white bars, exposed to different salinities. Superoxide dismutase (*SOD*) at 6 h (A), 48 h (B) and 6 d (C); *CAT* (catalase) D, E, F; and *DHAR* (dehydroascorbate reductase) G, H, I. Both populations were exposed to : 32 (control), 42, 62, 82 psu. Data correspond to mean ± SE (n = 3). Letters represent statistical differences at 95 % confidence interval (SNK test, $p < 0.05$).

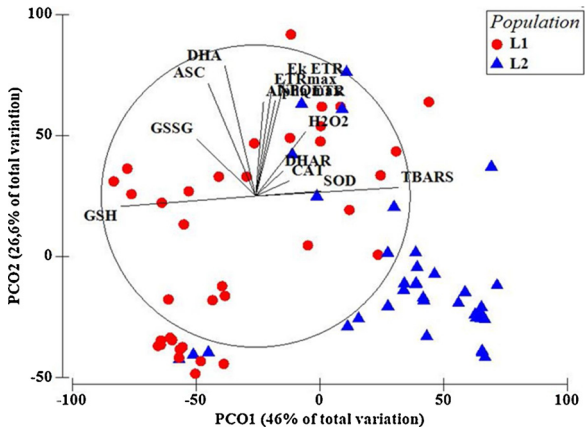

Fig. 7. Principal components ordination (PCO) analyses diagrams in *U. compressa* in relation to populations from Cachagua (L1) and Ventanas (L2). Both populations were exposed to hypersalinity salinity: 32 (control), 42, 62, 82 psu. Vectors overlay (Pearson correlation) indicate the relationship between the PCO axes and the parameters TBARS, H_2O_2, ASC (reduced ascorbate), DHA (oxizaded ascorbate), GSH (reduced glutathione), GSSG (oxizaded glutathione), maximum electron transport rate (ETR_{max}), photosynthetic efficiency ($Alpha_{ETR}$), saturation irradiance (Ek_{ETR}), maximum non-photochemical quenching (NPQ_{max}), expression genes dehydroascorbate reductase (*DHAR*), catalase (*CAT*) and superoxide dismutase (*SOD*).

electrons flow blockage within the PSII (Luo and Liu, 2011), as recorded in *U. compressa* especially from Ventanas. Even though it was not demonstrated an important threat to *U. compressa* viability at a physiological level considering oxidative stress responses and photosynthetic activity, the data showed that the population from Ventanas generally evidenced more signs of stress that individuals from Cachagua.

In regard to antioxidants, main patterns of increase were observed in *U. compressa* from Cachagua, starting at 42 psu after 6 h experiments, and later at the maximum salinity of 82 psu at 48 h and 6 d. Moreover, in both populations the trend at all times and at the highest salinities (mainly 82 psu) was an increase in DHA over ASC. It has been observed in photoautotrophs, including *U. compressa*, that an oxidative stress condition can mediate greater consumption of ASC, which is used as substrate of APX and oxidized to DHA, and therefore decreasing ASC/DHA ratio (Foyer and Noctor, 2011; Sáez et al., 2015c; Rodríguez-Rojas et al., 2019). In this regard, an investigation by Lu et al. (2006) in *U. fasciata* showed a rise of DHA in relation to ASC towards increasing salinities of up to ~90 psu. On the other hand, *U. prolifera* was not subject to changes in ASC up to 60 psu, although DHA was not measured (Luo and Liu, 2011). Considering other photoautotrophs, experiments from 0 of up to 24 psu the xero-halophyte desert plant *Haloxylon salicornicum* induced an increment in ASC/DHA ratios, demonstrating fast recycling and *de novo* synthesis of ASC under hypersalinity conditions (Panda et al., 2019). In terms of glutathione, while the population from Ventanas displayed a pattern of increasing total levels upon greater salinities only at 6 h, in the population from Cachagua that trend was observed at 48 h and 6 d. Moreover, although generally ratios of GSH/GSSG decreased with increasing salinities in both *U. compressa* populations, levels of GSH were always (over 70 %) higher than GSSG at all treatments and times. In this sense, it is known that GSH is involved in the defense system for scavenging H_2O_2, which it is used as an electron donor to reduce DHA to ASC by GR (Foyer and Noctor, 2011; Noctor et al., 2002). Thus, the information suggests that efficient GSH turnover observed in populations of *U. compressa* may be related to a proficient supply of DHA and GR activity. Also, GSH can also react non-enzymatically with singlet oxygen, superoxide and hydroxyl radicals through the oxidation of its thiol group (Noctor et al., 2002; Foyer and Noctor, 2011). In this context, Luo and Liu (2011) demonstrated that in *U. prolifera* a rapid accumulation total glutathione under ~60 psu after 6 d of exposition. Similarly, total glutathione was incremented after 7 d in *U. prolifera* and *U. intestinalis* when both species were exposed to high salinity of 35 psu versus 30 psu, although levels were much higher in *U. intestinalis* (Wang et al., 2012). In plants, Panda et al. (2019) found an increase in the GSH/GSSG ratio together with a raise of GR activity in *H. salicornicum* under high salinity (~18 and 24 psu) compared to controls (6 psu), suggesting efficient GR-mediated recycling of GSH. On the other hand, *de novo* biosynthesis of GSH occurs by two consecutive reactions catalyzed by γ-glutamyl-cysteine synthetase (γ-ECS) glutathione synthetase (GS) (Foyer and Noctor, 2011). In this regard, a salinity increase from 0 to 9 psu on the plant *Brassica napus* induced an increase in γ-ECS activity in parallel with greater concentration of GSH (Ruiz and Blumwald, 2002). Even though the participation of these enzymes has not been deeply addressed in macroalgae, recent investigations on *U. compressa* under copper excess demonstrated the increase in expression of a GS-encoding gene accompanied by higher levels of GSH (Rodríguez-Rojas et al., 2019). Thus, in terms of glutathione-ascorbate cycle, the information demonstrates hypersalinity-induced enhanced recycling and *de novo* syntheses of these antioxidants in *U. compressa*, although with intra-specific differences. Indeed, in spite that both populations maintained a sufficient batch and recycling of glutathione and ascorbate, in general the population of Cachagua appeared to better develop these processes compared to that from Ventanas.

In terms of genes expression of antioxidant enzymes (*SOD*, *CAT* and *DHAR*), differences were also observed between both populations of *U. compressa*. In contrast with ecophysiological and biochemical results, the expression of these enzymes under hypersalinity, at least at 48 h experiments and beyond, was shown with general patterns of upregulation in the population from Ventanas and downregulation in the individuals from Cachagua. The induction of enzymes involved in the antioxidant metabolism has been well documented in different photoautotroph under salinity excess. For example, Lu et al. (2006) demonstrated that *U. fasciata* above 60–90 psu for 4 d experiments had greater activities of the enzymes CAT, GR, APX. Similar results in the activities of CAT, SOD, GR and APX were observed in *U. prolifera* at 60 psu for 6 d (Luo and Liu, 2011). Related to expression, short-term experiment (less than 12 h) in *U. fasciata* at 90 psu observed the upregulation of the enzymes as Mn/Fe*SOD*, *APX*, *GR* and *CAT* also accompanied by greater activities; indeed, demonstrating transcriptional regulation in their activities (Sung et al., 2009). Moreover, the upregulation of genes encoding for *SOD*, *APX* and *CAT* was also observed in the red macroalga *Pyropia haitanensis* after 4 h at 110 psu (Wang et al., 2019). Although our results and the available literature demonstrates that salinity excess can induce the activation of antioxidant enzymes in different macroalgae species, our results demonstrates that a different environmental background can induce differential regulation in populations as observed in *U. compressa*. However, inter-population differences are also possible in the transcriptional regulation of the activities of these enzymes. In this regard, it is likely that although levels of expression of antioxidant enzymes is lower in the population from Cachagua than Ventanas, baseline levels of the enzyme and therefore their activities could be similar o even higher than in the latter; certainly, interesting subjects of for future investigations.

Ventanas houses several industries located in the shoreline, which have caused many environmental impacts associated with pollutants as metals (mainly copper) and hydrocarbons, with documented negative effects at different levels of biological organization (Durán et al., 2019; Sáez et al., 2015a, b; Sáez et al., 2012a). The accumulation of copper in *U. compressa* has been previously described, with concentration in its tissues being proportional to the levels in the environment (Ratkevicius et al., 2003). The capacity to cope with copper excess in *U. compressa* is well documented and it is known to be related with efficient mechanisms of cellular exclusion, chelation by metal-binding peptides as phytochelatins and metallothioneins, and the activation of antioxidant

defenses (Ratkevicius et al., 2003; Mellado et al., 2012; Moenne et al., 2016; Rodríguez-Rojas et al., 2019). To the extent of our knowledge, there are no published records addressing responses in populations exposed to stress after being collected from their polluted habitat of origin. However, our information on general lower biological performance and responses of *U. compressa* from Ventanas compared to the population from Cachagua may indicate, and to be empirically confirmed, is due to a baseline depressed basic and secondary metabolism mediated by a chronic long-term exposition to pollution-mediated stress.

5. Conclusion

This investigation represents the first attempt to investigate potential variations in response between different populations of macroalgae subject to salinity excess; moreover, considering different historical backgrounds of exposition to stress in native polluted environments. Although not affecting viability of any of the studied *U. compressa* populations, excess salinity did induce more signs of stress in the population of Ventanas manifested in lower photosynthetic performance and production of antioxidants glutathione and ascorbate. Instead, the expression of antioxidant enzymes appeared more favored in the population from Ventanas, although a transcriptional regulation in their activity remains to be confirmed. The information suggest that the population of *U. compressa* from Ventanas has baseline deteriorated biological metabolism that affects its responses to other sources of stress, as that induced by hypersalinty, confirming that the history of exposition to different stressor can mediate inter-population tolerance responses in green macroalgae.

CRediT authorship contribution statement

Pamela T. Muñoz: Conceptualization, Data curation, Formal analysis, Investigation, Methodology, Visualization, Writing - original draft, Writing - review & editing. **Fernanda Rodríguez-Rojas:** Data curation, Formal analysis, Funding acquisition, Writing - original draft, Writing - review & editing. **Paula S.M. Celis-Plá:** Formal analysis, Methodology, Writing - original draft, Writing - review & editing. **Lorena Méndez:** Data curation, Formal analysis, Visualization. **Denise Pinto:** Data curation, Formal analysis, Visualization. **Diego Pardo:** Data curation, Formal analysis, Visualization. **Fabiola Moenne:** Data curation, Formal analysis, Visualization, Project administration. **José Luis Sánchez-Lizaso:** Conceptualization, Data curation, Funding acquisition, Methodology, Writing - original draft, Writing - review & editing. **Claudio A. Sáez:** Conceptualization, Data curation, Funding acquisition, Investigation, Methodology, Writing - original draft, Writing - review & editing.

Declaration of Competing Interest

The authors declare that they have no known competing financial interests or personal relationships that could have appeared to influence the work reported in this paper.

Acknowledgments

The authors thank financial support of projects DGI RegularCEA 01-1819 and CEA 19-20, CORFO 19CTIGH-121349, and FONDECYT Postdoctorado3180394.

Appendix A. Supplementary data

Supplementary material related to this article can be found, in the online version, at doi:https://doi.org/10.1016/j.aquatox.2020.105552.

References

Aranda, P.S., LaJoie, D.M., Jorcyk, C.L., 2012. Bleach gel: a simple agarose gel for analyzing RNA quality. Electrophoresis 33 (2), 366–369.
Asada, K., 1999. The water-water cycle in chloroplasts: scavenging of active oxygens and dissipation of excess photons. Annu. Rev. Plant Biol. 50 (1), 601–639.
Bradford, M.M., 1976. A rapid and sensitive method for the quantitation of microgram quantities of protein utilizing the principle of protein-dye binding. Anal. Biochem. 72 (1), 248–254.
Celis-Plá, P.S., Rodríguez-Rojas, F., Méndez, L., Moenne, F., Muñoz, P.T., Lobos, M.G., Díaz, P., Sánchez-Lizaso, J.L., Brown, M.T., Moenne, A., 2019. MAPK pathway under chronic copper excess in green macroalgae (Chlorophyta): influence on metal exclusion/extrusion mechanisms and photosynthesis. Int. J. Mol. Sci. 20 (18), 4547.
Durán, R.E., Méndez, V., Rodriguez-Castro, L., Barra-Sanhueza, B., Salvà-Serra, F., Moore, E.R., Castro-Nallar, E., Seeger, M., 2019. Genomic and physiological traits of the marine bacterium *Alcaligenes aquatilis* QD168 isolated from Quintero Bay, Central Chile, reveal a robust adaptive response to environmental stressors. Front. Microbiol. 10 (528).
Eilers, P., Peeters, J., 1988. A model for the relationship between light intensity and the rate of photosynthesis in phytoplankton. Ecol. Modell. 42 (3–4), 199–215.
Fernández-Torquemada, Y., Gónzalez-Correa, J.M., Loya, A., Ferrero, L.M., Díaz-Valdés, M., Sánchez-Lizaso, J.L., 2009. Dispersion of brine discharge from seawater reverse osmosis desalination plants. Desalin. Water Treat. 5 (1–3), 137–145.
Figueroa, F.L., Conde-Álvarez, R., Gómez, I., 2003. Relations between electron transport rates determined by pulse amplitude modulated chlorophyll fluorescence and oxygen evolution in macroalgae under different light conditions. Photosyn. Res. 75 (3), 259–275.
Figueroa, F.L., Domínguez-González, B., Korbee, N., 2014. Vulnerability and acclimation to increased UVB radiation in three intertidal macroalgae of different morpho-functional groups. Mar. Environ. Res. 97, 30–38.
Foyer, C.H., Noctor, G., 2011. Ascorbate and glutathione: the heart of the redox hub. Plant Physiol. 155 (1), 2–18.
Garrote-Moreno, A., McDonald, A., Sherman, T.D., Sánchez-Lizaso, J.L., Heck, K.L., Cebrian, J., 2015. Short-term impacts of salinity pulses on ionic ratios of the seagrasses *Thalassia testudinum* and *Halodule wrightii*. Aquat. Bot. 120, 315–321.
Gill, S.S., Tuteja, N., 2010. Reactive oxygen species and antioxidant machinery in abiotic stress tolerance in crop plants. Plant Physiol. Biochem. 48 (12), 909–930.
Hajiboland, R., 2014. Reactive oxygen species and photosynthesis. Chapter 1 In: Ahmad, P. (Ed.), Oxidative Damage to Plants. Academic Press, San Diego, pp. 1–63.
Imlay, J.A., 2003. Pathways of oxidative damage. Ann. Rev. Microbiol. 57 (1), 395–418.
Kirst, G., 1990. Salinity tolerance of eukaryotic marine algae. Annu. Rev. Plant Biol. 41 (1), 21–53.
Kumar, M., Kumari, P., Reddy, C., Jha, B., 2014. Salinity and desiccation induced oxidative stress acclimation in seaweeds. Advances in Botanical Research 71. Elsevier, pp. 91–123.
Li, Y., Liu, J., Zhang, L., Pang, T., 2016. Changes of photosynthetic performances in mature thalli of the red alga *Gelidium amansii* (Gelidiaceae) exposed to different salinities. Mar. Biol. Res. 12 (6), 631–639.
Livak, K.J., Schmittgen, T.D., 2001. Analysis of relative gene expression data using real-time quantitative PCR and the $2-\Delta\Delta CT$ method. Methods 25 (4), 402–408.
Lu, I.-F., Sung, M.-S., Lee, T.-M., 2006. Salinity stress and hydrogen peroxide regulation of antioxidant defense system in *Ulva fasciata*. Mar. Biol. 150 (1), 1–15.
Luo, M.B., Liu, F., 2011. Salinity-induced oxidative stress and regulation of antioxidant defense system in the marine macroalga *Ulva prolifera*. J. Exp. Mar. Biol. Ecol. 409 (1–2), 223–228.
Marín-Guirao, L., Sandoval-Gil, J.M., Bernardeau-Esteller, J., Ruíz, J.M., Sánchez-Lizaso, J.L., 2013. Responses of the Mediterranean seagrass *Posidonia oceanica* to hypersaline stress duration and recovery. Mar. Environ. Res. 84, 60–75.
Mellado, M., Contreras, R.A., González, A., Dennett, G., Moenne, A., 2012. Copper-induced synthesis of ascorbate, glutathione and phytochelatins in the marine alga *Ulva compressa* (Chlorophyta). Plant Physiol. Biochem. 51, 102–108.
Moenne, A., González, A., Sáez, C.A., 2016. Mechanisms of metal tolerance in marine macroalgae, with emphasis on copper tolerance in Chlorophyta and Rhodophyta. Aquat. Toxicol. 176, 30–37.
Neaman, A., Reyes, L., Trolard, F., Bourrié, G., Sauvé, S., 2009. Copper mobility in contaminated soils of the Puchuncaví valley, central Chile. Geoderma 150 (3-4), 359–366.
Noctor, G., Gomez, L., Vanacker, H., Foyer, C.H., 2002. Interactions between biosynthesis, compartmentation and transport in the control of glutathione homeostasis and signalling. J. Exp. Bot. 53 (372), 1283–1304.
Ogawa, T., Ohki, K., Kamiya, M., 2013. Differences of spatial distribution and seasonal succession among *Ulva* species (Ulvophyceae) across salinity gradients. Phycologia 52 (6), 637–651.
Panda, A., Rangani, J., Kumar Parida, A., 2019. Cross talk between ROS homeostasis and antioxidative machinery contributes to salt tolerance of the xero-halophyte *Haloxylon salicornicum*. Environ. Exp. Bot. 166 (103799).
Ratkevicius, N., Correa, J.A., Moenne, A., 2003. Copper accumulation, synthesis of ascorbate and activation of ascorbate peroxidase in *Enteromorpha compressa* (L.) Grev. (Chlorophyta) from heavy metal-enriched environments in northern Chile. Plant Cell Environ. 26 (10), 1599–1608.
Rodríguez-Rojas, F., Celis-Plá, P.S., Méndez, L., Moenne, F., Muñoz, P.T., Lobos, M.G., Díaz, P., Sánchez-Lizaso, J.L., Brown, M.T., Moenne, A., 2019. MAPK pathway under chronic copper excess in green macroalgae (Chlorophyta): involvement in the regulation of detoxification mechanisms. Int. J. Mol. Sci. 20 (18), 4546.
Ruiz, J., Blumwald, E., 2002. Salinity-induced glutathione synthesis in *Brassica napus*.

Planta 214 (6), 965–969.
Rybak, A.S., 2018. Species of *Ulva* (Ulvophyceae, Chlorophyta) as indicators of salinity. Ecol. Indic. 85, 253–261.
Sáez, C.A., Lobos, M.G., Macaya, E.C., Oliva, D., Quiroz, W., Brown, M.T., 2012a. Variation in patterns of metal accumulation in thallus parts of *Lessonia trabeculata* (Laminariales; Phaeophyceae): implications for biomonitoring. PLoS One 7 (11), e50170.
Sáez, C.A., Pérez-Matus, A., Lobos, M.G., Oliva, D., Vásquez, J.A., Bravo, M., 2012b. Environmental assessment in a shallow subtidal rocky habitat: approach coupling chemical and ecological tools. Chem. Ecol. 28 (1), 1–15.
Sáez, C.A., González, A., Contreras, R.A., Moody, A.J., Moenne, A., Brown, M.T., 2015a. A novel field transplantation technique reveals intra-specific metal-induced oxidative responses in strains of *Ectocarpus siliculosus* with different pollution histories. Environ. Pollut. 199, 130–138.
Sáez, C.A., Ramesh, K., Greco, M., Bitonti, M.B., Brown, M.T., 2015b. Enzymatic antioxidant defences are transcriptionally regulated in Es524, a copper-tolerant strain of *Ectocarpus siliculosus* (Ectocarpales, Phaeophyceae). Phycologia 54 (4), 425–429.
Sáez, C.A., Roncarati, F., Moenne, A., Moody, A.J., Brown, M.T., 2015c. Copper-induced intra-specific oxidative damage and antioxidant responses in strains of the brown alga *Ectocarpus siliculosus* with different pollution histories. Aquat. Toxicol. 159, 81–89.
Sampath-Wiley, P., Neefus, C.D., Jahnke, L.S., 2008. Seasonal effects of sun exposure and emersion on intertidal seaweed physiology: fluctuations in antioxidant contents, photosynthetic pigments and photosynthetic efficiency in the red alga *Porphyra umbilicalis* Kützing (Rhodophyta, Bangiales). J. Exp. Mar. Biol. Ecol. 361 (2), 83–91.
Sandoval-Gil, J.M., Ruiz, J.M., Marín-Guirao, L., Bernardeau-Esteller, J., Sánchez-Lizaso, J.L., 2014. Ecophysiological plasticity of shallow and deep populations of the Mediterranean seagrasses *Posidonia oceanica* and *Cymodocea nodosa* in response to hypersaline stress. Mar. Environ. Res. 95, 39–61.
Schreiber, U., Bilger, W., Neubauer, C., 1995. Chlorophyll fluorescence as a nonintrusive indicator for rapid assessment of in vivo photosynthesis. Ecophysiology of Photosynthesis. Springer, Berlin, Heidelberg, pp. 49–70.
Sergiev, L., Alexieva, V., Karanov, E., 1997. Effect of spermine, atrazine and combination between them on some endogenous protective systems and stress markers in plants. Comptes rendus de l'Académie bulgare des Sciences 51, 121–124.
Sievers, H.A., Vega, S.A., 2000. Respuesta físico-química de la bahía de Valparaíso a la surgencia generada en punta Curaumilla y al fenómeno El Niño. Revista de biología marina y oceanografía 35, 153–168.
Ślesak, I., Ślesak, H., Zimak-Piekarczyk, P., Rozpądek, P., 2016. Enzymatic antioxidant systems in early anaerobes: theoretical considerations. Astrobiology 16 (5), 348–358.
Sola, I., Sánchez-Lizaso, J.L., Muñoz, P.T., García-Bartolomei, E., Sáez, C.A., Zarzo, D., 2019a. Assessment of the requirements within the environmental monitoring plans used to evaluate the environmental impacts of desalination plants in Chile. Water 11 (10), 2085.
Sola, I., Zarzo, D., Sánchez-Lizaso, J.L., 2019b. Evaluating environmental requirements for the management of brine discharges in Spain. Desalination 471, 114132.
Sung, M.-S., Hsu, Y.-T., Hsu, Y.-T., Wu, T.-M., Lee, T.-M., 2009. Hypersalinity and hydrogen peroxide upregulation of gene expression of antioxidant enzymes in *Ulva fasciata* against oxidative stress. Mar. Biotechnol. 11 (2), 199.
Tine, M., de Lorgeril, J., D'Cotta, H., Pepey, E., Bonhomme, F., Baroiller, J.F., Durand, J.-D., 2008. Transcriptional responses of the black-chinned tilapia *Sarotherodon melanotheron* to salinity extremes. Mar. Genom. 1 (2), 37–46.
Tume, P., Barrueto, K., Olguin, M., Torres, J., Cifuentes, J., Ferraro, F.X., Roca, N., Bech, J., Cornejo, O., 2019. The Influence of the Industrial Area on the Pollution Outside Its Borders: a Case Study From Quintero and Puchuncaví Districts. Environmental Geochemistry and Health, Chile.
Vargas-Chacoff, L., Saavedra, E., Oyarzún, R., Martínez-Montaño, E., Pontigo, J.P., Yáñez, A., Ruiz-Jarabo, I., Mancera, J.M., Ortiz, E., Bertrán, C., 2015. Effects on the metabolism, growth, digestive capacity and osmoregulation of juvenile of Sub-Antarctic Notothenioid fish *Eleginops maclovinus* acclimated at different salinities. Fish Physiol. Biochem. 41 (6), 1369–1381.
Wang, Y., Wang, Y., Zhu, L., Zhou, B., Tang, X., 2012. Comparative studies on the ecophysiological eifferences of two green tide macroalgae under controlled laboratory conditions. PLoS One 7 (8), e38245.
Wang, W., Xu, Y., Chen, T., Xing, L., Xu, K., Ji, D., Chen, C., Xie, C., 2019. Regulatory mechanisms underlying the maintenance of homeostasis in *Pyropia haitanensis* under hypersaline stress conditions. Sci. Total Environ. 662, 168–179.
Xia, J., Li, Y., Zou, D., 2004. Effects of salinity stress on PSII in *Ulva lactuca* as probed by chlorophyll fluorescence measurements. Aquat. Bot. 80 (2), 129–137.